Pyramidal Cell Selective Ablation of *N*-Methyl-D-Aspartate Receptor 1 Causes Increase in Cellular and Network Excitability

Supplemental Information

Supplementary Methods

Animal Husbandry

Animals were housed in temperature-controlled rooms with a 12-hour light/12-hour dark cycle (lights on at 7:00 AM). They were given TestDiet 5001 (Purina Mills, Richmond, Indiana) and water *ad libitum*. Cages were changed weekly. All animal procedures were in strict accordance with the National Institutes of Health Guide for the Care and Use of Laboratory Animals and were approved by the University of Pennsylvania Institutional Animal Care and Use Committee.

Breeding Strategy

Homozygous Camk2αCre/Cre mice (B6.Cg-Tg(Camk2α-cre)T29-1Stl/J), homozygous NMDA-R1Flox/Flox mice (B6.129S4-*Grin1*^{tm2Stl}/J) and heterozygous cre reporter mice (B6;129S6-*Gt(ROSA)26Sor*$^{tm14(CAG-tdTomato)Hze}$/J) were obtained from The Jackson Laboratory (Bar Harbor, Maine). The Camk2αCre/Cre mice and the NMDA-R1Flox/Flox mice were bred in order to obtain the following genotypes: Camk2αCre/Cre;NMDA-R1+/+ (referred as Camk2αCre-WT) and Camk2αCre/Cre; NMDA-R1Flox/Flox (referred as Camk2αCre-cKO).

Homozygous Camk2αCre/Cre mice were also bred with the cre reporter mice that harbor a targeted mutation of the *Gt(ROSA)26Sor* locus with a *loxP*-flanked STOP cassette preventing transcription of a CAG promoter-driven red fluorescent protein variant (tdTomato). As a consequence, (td)Tomato is expressed following Cre-mediated recombination. These mice are referred as Camk2αCre-WT;(td)TomatoFlox (where NMDA-R1 is not knocked out) and

Camk2αCre-cKO;(td)TomatoFlox mice (where NMDA-R1 is knocked out). Experiments were performed on males only between the ages of 3 to 6 months.

Tissue Preparation

For in situ hybridization, Camk2αCre-cKO and their Camk2αCre-WT littermates were intracardially perfused with 10 mL of ice-cold saline solution followed by 30 mL of ice-cold 10% buffered formalin solution. Brains were dissected and post-fixed overnight in 10% buffered formalin solution at 4°C. Brains were cryoprotected by incubation in PBS1X containing increasing concentration of sucrose (10%, 20% and 30%), for 24 hours each, after which they were frozen in isopentane on dry ice and stored at -80°C. Fifty micron sections were cut and stored in a cryoprotective solution (30% sucrose, 30% ethylene glycol in PBS1X) at -20°C until processing. For western blot and RNA analysis, brains were surgically removed and hippocampus and cortex of each hemisphere were isolated and frozen on dry ice.

In Situ Hybridization

Riboprobe Synthesis: Total RNA was extracted from frozen murine brain tissues using Trizol (Invitrogen), treated with DNase I (Promega) then reverse transcribed using Superscript II reverse transcriptase according to the manufacturer's instructions (Invitrogen). cDNA fragment corresponding to *Grin1* was cloned by polymerase chain reaction (PCR) amplification using the following primers: Forward 5'-CCATGGACGGGGCCTAATGACACA-3' and Reverse 5'GTCGACATGGCCT CAGCTGCACTC-3'. The amplified fragment was cloned into the pGEMT easy vector (Promega). Digoxigenin-labeled antisense riboprobe was obtained by in vitro transcription using SP6 transcriptase (Promega) and digoxigenin-UTP (Roche).

In Situ Hybridization on Frozen Floating Sections: The sections were washed in PBS, then RIPA buffer (NaCl 150 mM, NP-40 1%, sodium deoxycholate 0.05%, SDS 0.1%, EDTA 1 mM pH = 8, Tris-HCl 50 mM pH = 8) and post-fixed in 4% PFA for 5 min before being treated

with 0.25 acetic anhydre in 0.1 M of triethanolamine. Hybridization was performed with digoxigenin-labeled antisense riboprobe overnight at 70°C in hybridization buffer. The sections were washed with 50% formamide/2X SSC/0.1%, Tween 20 for 2 h at 70°C then MABT at room temperature. After blocking with 10% goat serum/MABT, hybridization was revealed by incubation with an alkaline phosphatase coupled antibody (Roche, dilution 1:1,000 in MABT, 10% heat-inactivated goat serum blocking buffer) overnight at 4°C. The slides were washed with MABT and with alkaline phosphatase buffer. The sections were then incubated in a 5-bromo-4-chloro-3-indolyl phosphate/nitroblue tetrazolium solution (Sigma).

Post-synaptic Density Fractionation: Cortex tissues from Camk2αCre-cKO and Camk2αCre-WT mice were surgically removed and stored at -80°C. They were homogenized in a homogenization buffer (0.32 M sucrose, 10 mM Tris pH = 7.5, 1 mM EDTA, 1 mM EGTA) and submitted to a fractionation protein extraction protocol (1). The cortical homogenate was centrifuged at 1000 *g* for 10 min at 4°C to obtain the nuclear fraction in the pellet (P1). The supernatant (S1) was centrifuged at 10,000 *g* 15 min and the supernatant (S2) contained cytosol fraction (S2). The pellet P2 was resuspended in sucrose homogenization buffer and 8 volumes of Triton-X buffer (1% Triton-X100, 10 mM Tris pH = 8, 1 mM EDTA, 1 mM EGTA) were added. The homogenate was incubated at 4°C rotating for 20 min before being ultracentrifuged (Beckman L-65 ultracentrifuge, 50.4ti rotor, 36,000 rpm for 20 min). The resulting P3 pellet was resuspended in Triton-X buffer, sonicated and incubated at 4°C for 20 min. The resulting homogenate was ultracentrifuged (36,000 rpm for 30 min) at 4°C and the pellet (P4) which contained the PSD fraction was resuspended in 25 mM trisHCl pH 7.4 supplemented with 1% SDS, mixed for 15 min and sonicated for 15 min. Protein extracts (20 µg) were loaded onto NuPage Novex 4-12% Bis-Tris precast gels (Invitrogen) and transferred onto PVDF membrane (Millipore). The membrane was blocked in 3% nonfat milk and probed overnight at 4°C with the following antibodies: anti $GABA_{B2}$ receptor (1:1000, rabbit polyclonal, CST 3839) or anti GIRK2 (1:100, rabbit polyclonal, AB30738, Abcam) and anti-β-Actin (1:50000,

mouse monoclonal, AB6276, Abcam), followed by secondary antibodies goat anti-mouse (12-349, Millipore), donkey anti-rabbit (711-035-152, Jackson). Blots were developed with chemiluminescence reagent ECL (Thermo Scientific). Films were scanned with a GS-800 Calibrated Densitometer and the signal was quantified using the Quantity One 4.6.3 software.

RNA Analysis: RNAs from hippocampus, cortex and striatum were purified from tissues using Trizol. High Capacity cDNA Reverse Transcription Kit (Applied Biosystems) was used for reverse transcription, as recommended by the manufacturer. Quantitative PCR was performed using *Power* SYBR® Green PCR Master Mix (Applied Biosystems) as recommended by the manufacturer. The primer pairs shown in Table S1 were used for amplification.

Patch Clamp: Picrotoxin (100 µM) was added to all solutions to block the $GABA_A$ receptor-mediated currents. The intracellular solution contained (mM): 145 potassium gluconate, 2 $MgCl_2$, 2.5 KCl, 2.5 NaCl, 0.1 BAPTA, 10 HEPES, 2 Mg-ATP, 0.5 GTP-Tris (pH 7.2–7.3 with KOH, osmolarity 280–290 mOsm). Recordings were performed in whole-cell voltage-clamp (Vh = -65 mV) or whole-cell current-clamp (at resting potential) modes as indicated. The data were acquired through a MultiClamp700B amplifier (Molecular Devices). Currents were low-pass filtered at 2 kHz and digitized at 20 kHz using a Digidata 1440A acquisition board and pClamp10 software (both from Molecular Devices). Access resistance was monitored throughout the recordings by injection of 10 mV hyperpolarizing pulses (in voltage-clamp) and data was discarded if the access resistance changed by >25% over the course of data acquisition. Spikes were triggered with 500 ms rectangular current pulse injection using pClamp 10 software. Evoked responses were triggered by constant-current pulses generated by an A310 Accupulser (World Precision Instruments) and delivered at 0.2 Hz via a bipolar tungsten stimulation electrode positioned within 100 µm of the recorded cell. The amplitude of the current pulses was controlled by a stimulus isolator (ISO-Flex, A.M.P.I.) and was adjusted in each cell to evoke a minimal response with a 25 µs current pulse. The current duration was then increased to 50, 75, 100, 125 and 150 µs to construct an input-output curve

for the evoked synaptic events. For AMPA/NMDA ratio experiments Camk2αCre-WT;(td)TomatoFlox and Camk2αCre-cKO;(td)TomatoFlox mice were used in order to specifically visualize the pyramidal cells. Picrotoxin (100 µM) was added to extracellular solutions to block the $GABA_A$ receptor-mediated currents and D-serine (10 µM) to facilitate NMDA receptor activity. The intracellular solution contained (in mM): 100 $CsCH_3O_3S$, 50 CsCl, 3 KCl, 0.2 BAPTA, 10 HEPES, 1 $MgCl_2$, 2.5 phosphocreatine-2Na, 2 Mg-ATP, 0.25 GTP-Tris, 1 QX-314, adjusted to pH 7.2–7.3 (pH 7.2–7.3 with CsOH, osmolarity 280–290 mOsm). We evoked excitatory postsynaptic currents (EPSCs) by stimulating Schaffer collateral axons. The AMPAR component was measured at the peak of the EPSC at −70 mV, whereas the NMDAR component was measured at 50 ms after stimulus at +40 mV. To reduce polysynaptic responses and spontaneous bursting activity, the dentate gyrus and the CA3 were cut from the slices. All analyses of intracellular recordings were carried out with Clampfit 10 (Molecular Devices). Spontaneous EPSC amplitudes were computed from averages of at least 20 spontaneous EPSC traces. Mean spontaneous EPSC frequencies were analyzed from 5–200 s long trace segments. Evoked EPSC amplitudes were computed from an average of 5-10 responses at each stimulation intensity. Rheobase was measured as the minimal current (advanced in 10 pA steps) necessary to trigger an action potential.

Long-Term Potentiation: For long-term potentiation (LTP) studies, the trigger and recording electrodes were placed in the stratum radiatum in CA1. Evoked responses were triggered by constant-current pulses generated by an A310 Accupulser (World Precision Instruments) and delivered at 50% of maximum stimulus via a bipolar tungsten stimulation electrode positioned within 100 µm of the recording electrode. Baseline stimulation was recorded for 15 minutes prior to onset of tetanus. Tetanus was induced by giving two 100 Hz pulses 10 seconds apart. LTP was recorded for an hour.

Electroencephalography Recording: Recording of auditory event-related potentials was performed on awake mice at least 1 week after electrode implantation, in a home-cage

environment, as previously described (2-5). Mice were brought to the room 30 minutes prior to recording for acclimation. Cages were placed in a sound attenuated recording chamber located inside a Faraday electrical isolation cage. Electrode pedestals were connected to a 30 cm tripolar electrode cable that exited the chamber to connect to a high impedance differential AC amplifier (A-M Systems, Carlsborg, WA, USA). Stimuli were generated by Micro1401 hardware with Spike2 software (Cambridge Electronic Design, Cambridge, UK) and were delivered through speakers attached to the cage top. The sequencer file consisted of a series of 200-paired white-noise stimuli at 85 dB with 8 seconds inter-stimulus interval. Raw electroencephalography (EEG) was filtered between 1 and 500 Hz. Individual sweeps were rejected for movement artifact based on a criterion of 2 times the root mean squared amplitude per mouse.

Signal Processing: Time-frequency decomposition of EEG signal was performed with the EEGLAB toolbox in MATLAB (6). Single trial epochs between -1 and 1 second relative were extracted from the continuous data sampled at 1667 Hz. Baseline power and evoked (i.e., phase-locked) power were calculated using Morlet wavelets in 100 linearly spaced frequency bins between 5-100 Hz, with wavelet cycles linearly increasing from 3 to 6, as published (7). For each subject, evoked power was averaged from 0-50 ms post-stimulus in gamma frequency range (30-80 Hz). Pre-stimulus total power was calculated in the same frequency ranges from -400 to -100 ms relative to the stimulus onset. Gamma signal-to-noise ratio was calculated as the evoked gamma-band response divided by the pre-stimulus baseline gamma power.

Social Interactions: A three chamber testing apparatus with a clean mat and clean mouse bedding was used. Two identical clear cylinders with small holes were placed in each end. A stimulus mouse was placed in one cylinder (social cylinder) while the other cylinder contained an inanimate object (non-social cylinder). The test mouse was transferred to the middle chamber and allowed to explore the apparatus for five minutes. The time spent smelling

each cylinder as well as the number of times the test mouse sniffed each cylinder were calculated. The apparatus was thoroughly cleaned between each test.

Self-care Behaviors: Briefly, mice housed in groups were transferred to single cages containing clean bedding, approximately one hour before the dark cycle. Three grams of non-shredded Nestlet was added to each cage. The following morning, pictures of the nests were taken. The weights of unturned Nestlet as well as the dispersion of Nestlets pieces in the cage were determined. A score of zero was given to an unturned Nestlet while a score of 5 was given to a fully turned, undispersed Nestlet.

Cognitive Behaviors: Mice were brought to the test room 30 minutes before testing to acclimate. Soiled bedding from the opposite sex was disposed in the maze as previously described (8). The bedding was changed between each set of trials. Mice were tracked with an overhead video camera and manually scored. Briefly, a mouse was scored as having entered an arm when all four paws were located within the runway. For discrete trials, all three doors of the maze were raised and the central partition put in place. Each individual mouse was placed at the end of the start arm facing away from goal arms. Once the mouse had reached the goal arm, the door was shut quietly and the mouse was left to explore for 30 seconds. Afterwards, the central partition was removed, all doors were raised and the mouse was returned to the start arm and allowed to choose between the 2 opened goal arms. A cut-off time of 90 seconds was used for sample or choice runs. The mouse was considered to have alternated if it had chosen the opposite arm as the one chosen during the first run. For continuous trials, an alternation was defined as sequential entries into each of the three different arms (e.g., ABC, BCA, etc.). As such, a non-alternation behavior occurred when a mouse re-entered an arm that it had visited in the previous trial (e.g., BAB, CBC, etc.). Spontaneous alternation percentage was calculated as the total number of alternations divided by (total arm entries – 2) (9).

Open Field: The walls were free of any cues and the bottom of the box was cleaned with ethanol 70% between each mouse. Animals were allowed to habituate for 30 minutes in a room

that was illuminated with the same white light intensity as the housing room. After the habituation period, mice were transferred to a clear photobeam activity system that utilizes a 16x16 photobeam configuration, with a 1" space between the beams (San Diego Instruments, San Diego, CA). The system is composed of stainless steel frames and a clear plastic animal enclosure measuring 16"(W)x16"(D)x15"(H). The test ran for 30 minutes during which the total distance traveled was recorded using the MED PC software set to record the number of times that horizontal light beams were broken.

Ex-Vivo Electrophysiology: The brain was removed and coronal slices (300 μm thick) containing the hippocampus were cut with Vibratome (VT1000S, Leica Microsystems) in an ice-cold cutting solution containing (in mM): 3 KCl, 1.25 NaH_2PO_4, 26 $NaHCO_3$, 10 glucose, 219 sucrose, 1 $MgCl_2$, 2 $CaCl_2$ and 1 L-ascorbic acid, and saturated with 95% O_2/5% CO_2. Slices were incubated in artificial cerebrospinal fluid (ACSF) at 32–34°C for 30 min and kept at 22-25°C thereafter, until transfer to the recording chamber. Slices were viewed using infrared differential interference contrast optics under an upright microscope (Eclipse FN1, Nikon Instruments Inc.) with a 40x water-immersion objective. The recording chamber was continuously perfused (1–2 ml/min) with ACSF saturated with 95% O_2/5% CO_2 and heated to 32±1°C using an automatic temperature controller (Warner Instruments). Patch clamp and LTP recordings were performed as described above.

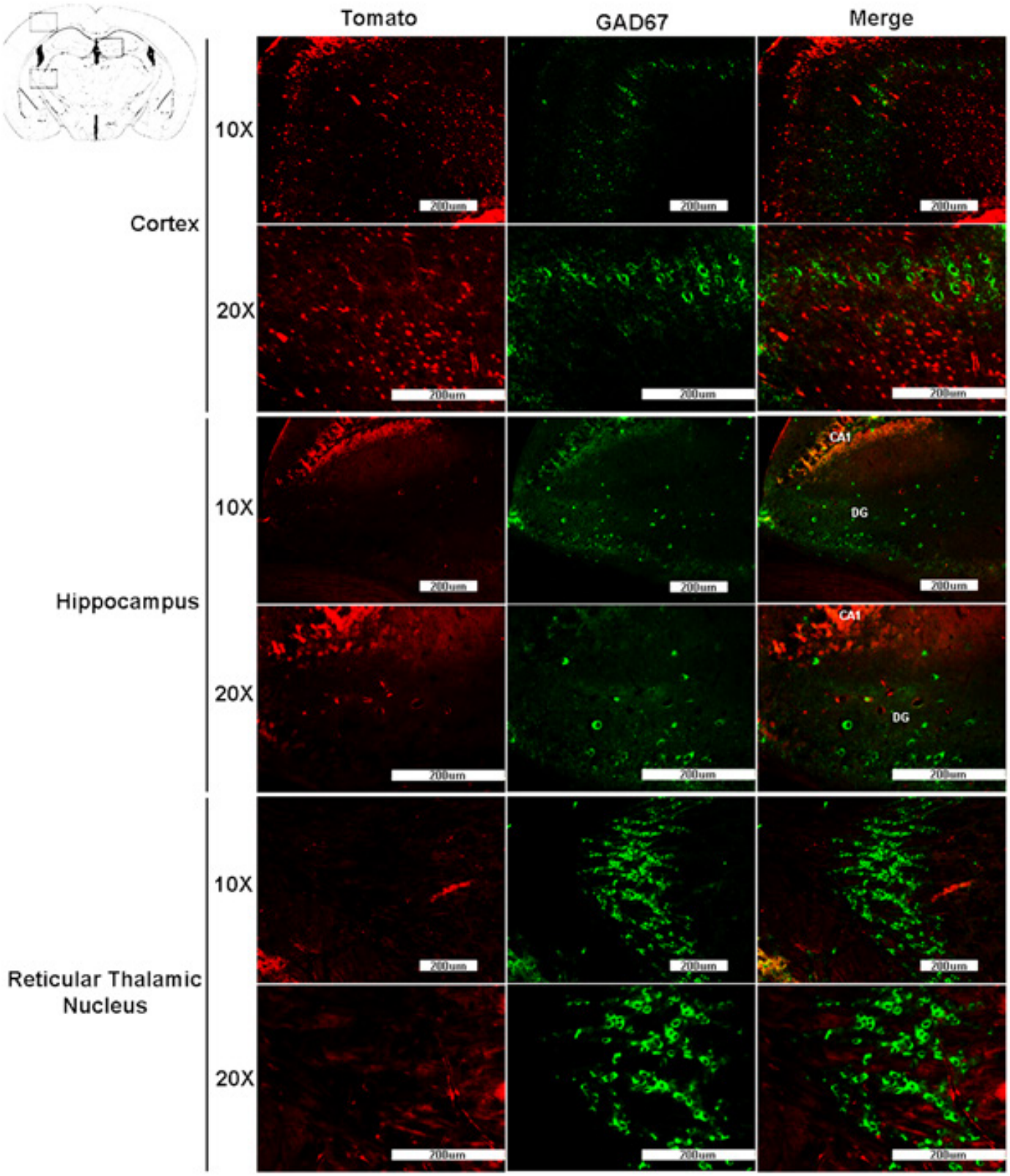

Figure S1. Cre recombination does not occur in GABAergic interneurons. The top left schema shows the area where the pictures were taken on a brain section. Red = (td)Tomato (Cre expression/recombination) and Green = GAD67. There is not superposition of signal between (td)Tomato and GAD67 in the cortex (top panel), hippocampus (middle panel) or reticular thalamic nucleus (bottom panel).

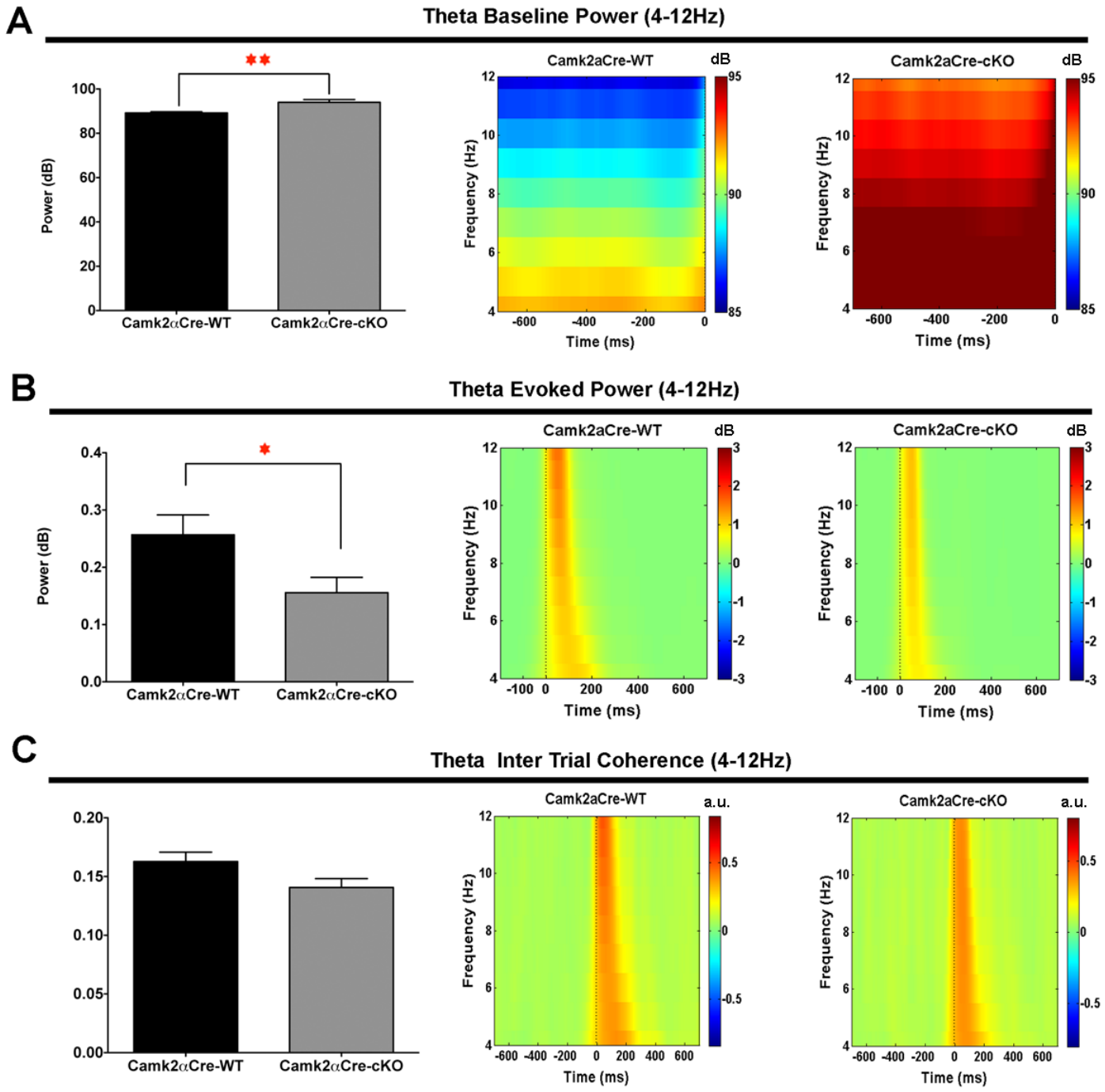

Figure S2. Theta band oscillatory activity is disrupted in pyramidal neuron specific NMDA-R1 KO mice. (A) Camk2αCre-cKO mice show a significant increase in baseline theta power compared to the wild type mice recorded from -700 ms to 0 ms before the stimulus (Camk2αCre-WT = 89.18 ± 0.51 dB, n = 17; Camk2αCre-cKO = 93.94 ± 1.26 dB, n = 16; p = 0.002, t = 3.50). **(B)** Evoked theta power, measured within 700 ms following the stimulus, was decreased in the Camk2αCre-cKO compared to the Camk2αCre-WT mice (Camk2αCre-WT = 0.26 ± 0.03 dB, n = 17; Camk2αCre-cKO = 0.16 ± 0.03 dB, n = 16; p = 0.028, t = 2.31). **(C)** The inter-trial coherence representing the level of synchrony of oscillatory activity between trials at theta band frequency was qualitatively, but not significantly decreased in Camk2αCre-cKO mice (Camk2αCre-WT = 0.162 ± 0.01, n = 17; Camk2αCre-cKO = 0.140 ± 0.01, n = 16; p = 0.0547, t = 1.99). Statistical analyses were performed using an unpaired two tailed t-test followed by Welch's post-hoc when appropriate **(A)**, to correct for unequal variance. Significance after Bonferroni correction requires p = 0.006. (*p < 0.05, **p < 0.01).

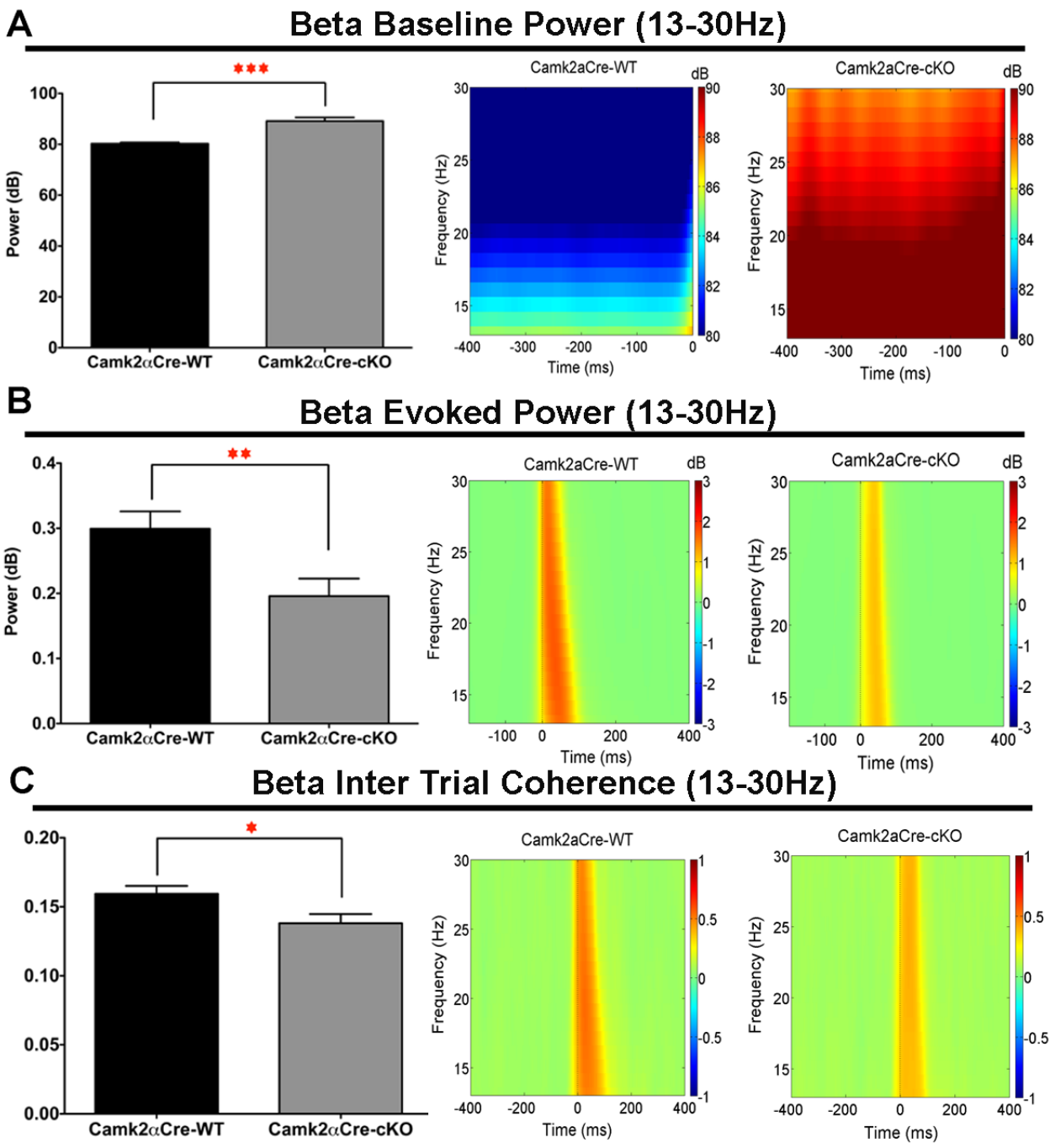

Figure S3. Beta band oscillatory activity is disrupted in pyramidal neuron specific NMDA-R1 KO mice. (A) Camk2αCre-cKO mice show a significant increase in baseline beta power compared to the wild type mice recorded from -700 ms to 0 ms before the stimulus (Camk2αCre-WT = 80.23 ± 0.50 dB, n = 17; Camk2αCre-cKO = 89.15 ± 1.41 dB, n = 16; $p < 0.0001$, $t = 5.96$). **(B)** Evoked theta power, measured within 700 ms following the stimulus, was decreased in the Camk2αCre-cKO compared to the Camk2αCre-WT mice (Camk2αCre-WT = 0.299 ± 0.03 dB, n = 17; Camk2αCre-cKO = 0.196 ± 0.03 dB, n = 16; $p = 0.0105$, $t = 2.73$). **(C)** The inter-trial coherence representing the level of synchrony of oscillatory activity between trials at theta band frequency was qualitatively, but not significantly decreased in Camk2αCre-cKO mice (Camk2αCre-WT = 0.159 ± 0.01, n = 17; Camk2αCre-cKO = 0.138 ± 0.01, n = 16; $p = 0.022$, $t = 2.41$). Statistical analyses were performed using an unpaired two tailed t-test followed by Welch's post-hoc when appropriate **(A)**, to correct for unequal variance. Significance after Bonferroni correction requires $p = 0.006$. (*$p < 0.05$, **$p < 0.01$, ***$p < 0.001$).

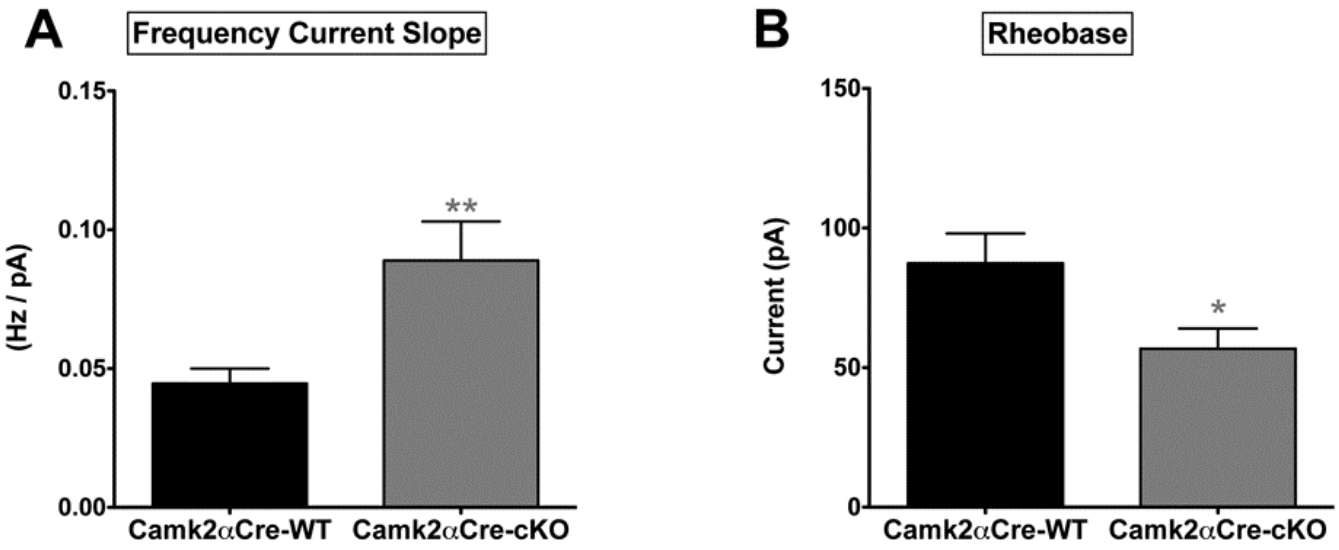

Figure S4. Measures of pyramidal neuron electrophysiological activity. (A) Loss of NMDA-R1 in pyramidal neurons led to an increase in the frequency-current slope depicting the increase in firing frequency in the Camk2αCre-cKO mice compared to their wild type littermates (Camk2αCre-WT = 0.045 ± 0.005 Hz/pA, n = 13; Camk2αCre-cKO = 0.089 ± 0.014 Hz/pA, n = 13; p = 0.01, t = 2.937). **(B)** There was also an increase in rheobase in the pyramidal neurons of the Camk2αCre-cKO mice compared to the Camk2αCre-WT mice, consistent with an increase in pyramidal cell excitability (Camk2αCre-WT = 87.36 ± 10.71 pA, n = 13; Camk2αCre-cKO = 56.79 ± 7.229 pA, n = 13; p = 0.028, t = 2.365). Statistical analyses in **(A)** and **(B)** were performed using an unpaired two tailed t-test followed by Welch's post-hoc when appropriate **(A)** to correct for unequal variance. Significance after Bonferroni correction requires p = 0.007. (*p < 0.05, **p < 0.01).

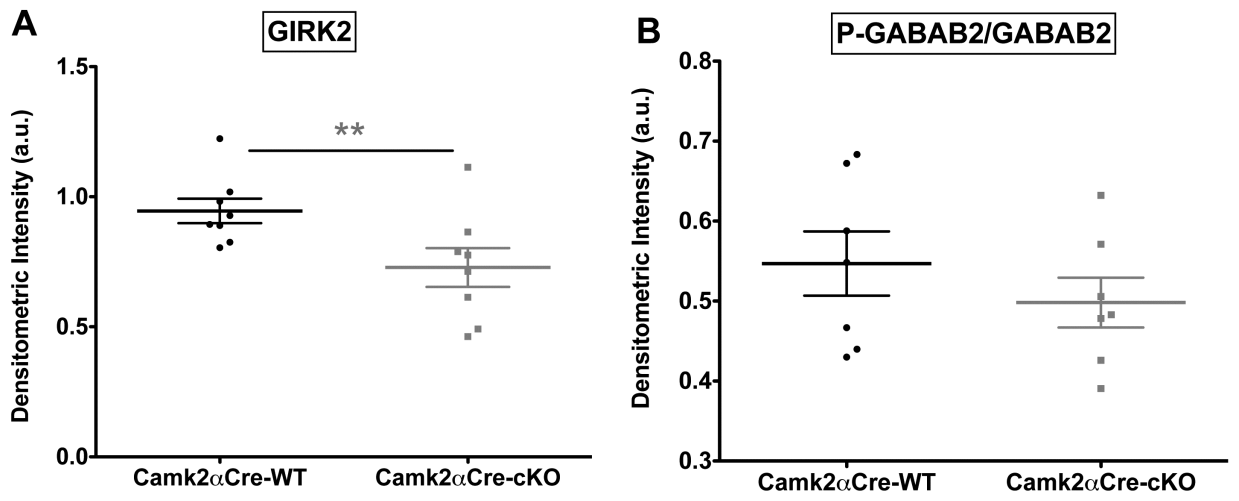

Figure S5. Decrease in GIRK2 channel as a possible mechanism for increased pyramidal neuron excitability. (A) GIRK2 expression in Camk2αCre-cKO mice is significantly decreased compared to the WT mice (Camk2αCre-WT = 0.94 ± 0.05 a.u., *n* = 8; Camk2αCre-cKO = 0.73 ± 0.07 a.u., *n* = 8; *p* = 0.015, Mann-Whitney, two-tailed). **(B)** The activation of the $GABA_{B2}$ receptor as shown by the ratio of phopsho-S783$GABA_{B2}$/$GABA_{B2}$ was determined by western blot in the postsynaptic density fraction of cortical extract from both groups of mice. No difference in activation was observed between the two genotypes (Camk2αCre-WT = 0.55 ± 0.04 a.u., *n* = 7; Camk2αCre-cKO = 0.50 ± 0.03 a.u., *n* = 7; *p* = 0.456, Mann-Whitney, two-tailed). (**$p < 0.01$).

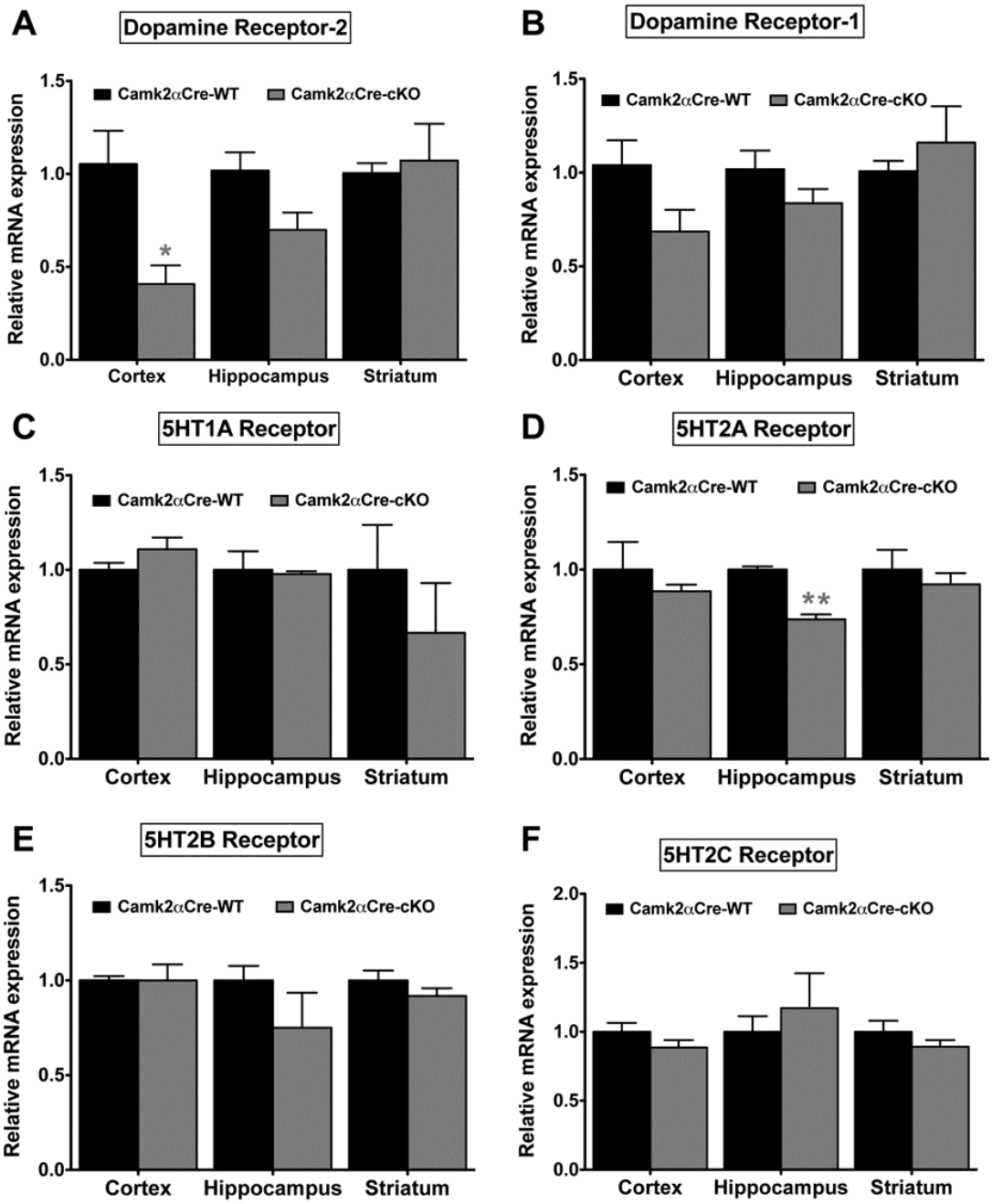

Figure S6. Dopaminergic and serotoninergic systems are affected in Camk2αCre-cKO mice. **(A, B)** Dopamine receptor mRNA expression in the cortex, hippocampus and striatum: **(A)** DRD2 mRNA expression is significantly decreased in the neocortex of Camk2αCre-cKO mice compared to the Camk2αCre-WT mice. **(B)** DRD1 mRNA expression is also qualitatively decreased but the change does not reach statistical significance. (**Cortex**: DRD2: Camk2αCre-WT = 1.05 ± 0.18, *n* = 6; Camk2αCre-cKO = 0.41 ± 0.1, *n* = 6; *p* = 0.015; DRD1: Camk2αCre-WT = 1 ± 0.14, *n* = 7; Camk2αCre-cKO = 0.69 ± 0.11, *n* = 7; *p* = 0.073; **Hippocampus**: DRD2: Camk2αCre-WT = 1.02 ± 0.1, *n* = 7; Camk2αCre-cKO = 0.7 ± 0.1, *n* = 7; *p* = 0.053; DRD1: Camk2αCre-WT = 1 ± 0.22, *n* = 7; Camk2αCre-cKO = 0.84 ± 0.07, *n* = 7; *p* = 0.318; **Striatum**: DRD2: Camk2αCre-WT = 1 ± 0.05, *n* = 7; Camk2αCre-cKO = 1.1 ± 0.2, *n* = 7; *p* = 0.805; DRD1: Camk2αCre-WT = 1 ± 0.05, *n* = 7; Camk2αCre-cKO = 1.16 ± 0.19, *n* = 7; *p* = 0.456, Mann-Whitney, two tailed, all samples were run in duplicate). **(C-F)** Serotonin receptor 5HT1A and 5HT2A-C expression in cortex, hippocampus and striatum. Expression of serotonin receptors was quantified by real time PCR. Only the expression of 5HT2A receptors was significantly decreased in the hippocampus of Camk2αCre-cKO mice. None of

the other serotonin receptors was significantly changed. (**Cortex:** 5HT1A: Camk2αCre-WT = 1.0 ± 0.04, *n* = 4; Camk2αCre-cKO = 1.11 ± 0.06, *n* = 4; *p* = 0.486. 5HT2A: Camk2αCre-WT = 1.0 ± 0.15, *n* = 5; Camk2αCre-cKO = 0.89 ± 0.03, *n* = 5; *p* = 1. 5HT2B: Camk2αCre-WT = 1.0 ± 0.02, *n* = 5; Camk2αCre-cKO = 1.0 ± 0.08, *n* = 5; *p* = 0.421. 5HT2C: Camk2αCre-WT = 1.0 ± 0.06, *n* = 5; Camk2αCre-cKO = 0.89 ± 0.05, *n* = 5; *p* = 0.309; **Hippocampus:** 5HT1A: Camk2αCre-WT = 1.0 ± 0.1, *n* = 5; Camk2αCre-cKO = 1.0 ± 0.01, *n* = 5; *p* = 1. 5HT2A: Camk2αCre-WT = 1.0 ± 0.2, *n* = 5; Camk2αCre-cKO = 0.74 ± 0.03, *n* = 5; *p* = 0.008. 5HT2B: Camk2αCre-WT = 1 ± 0.08, *n* = 5; Camk2αCre-cKO = 0.75 ± 0.18, *n* = 5; *p* = 0.309. 5HT2C: Camk2αCre-WT = 1.0 ± 0.11, *n* = 5; Camk2αCre-cKO = 1.12 ± 0.25, *n* = 5; *p* = 0.841; **Striatum:** 5HT1A: Camk2αCre-WT = 1.0 ± 0.24, *n* = 5; Camk2αCre-cKO = 0.67 ± 0.26, *n* = 5; *p* = 0.151. 5HT2A: Camk2αCre-WT = 1 ± 0.10, *n* = 5; Camk2αCre-cKO = 0.92 ± 0.06, *n* = 5; *p* = 1. 5HT2B: Camk2αCre-WT = 1.0 ± 0.05, *n* = 5; Camk2αCre-cKO = 0.92 ± 0.04, *n* = 5; *p* = 0.309. 5HT2C: Camk2αCre-WT = 1.0 ± 0.08, *n* = 5; Camk2αCre-cKO = 0.89 ± 0.05, *n* = 5; *p* = 0.841. Mann-Whitney, two tailed, all samples were run in duplicate). (*$p < 0.05$, **$p < 0.01$).

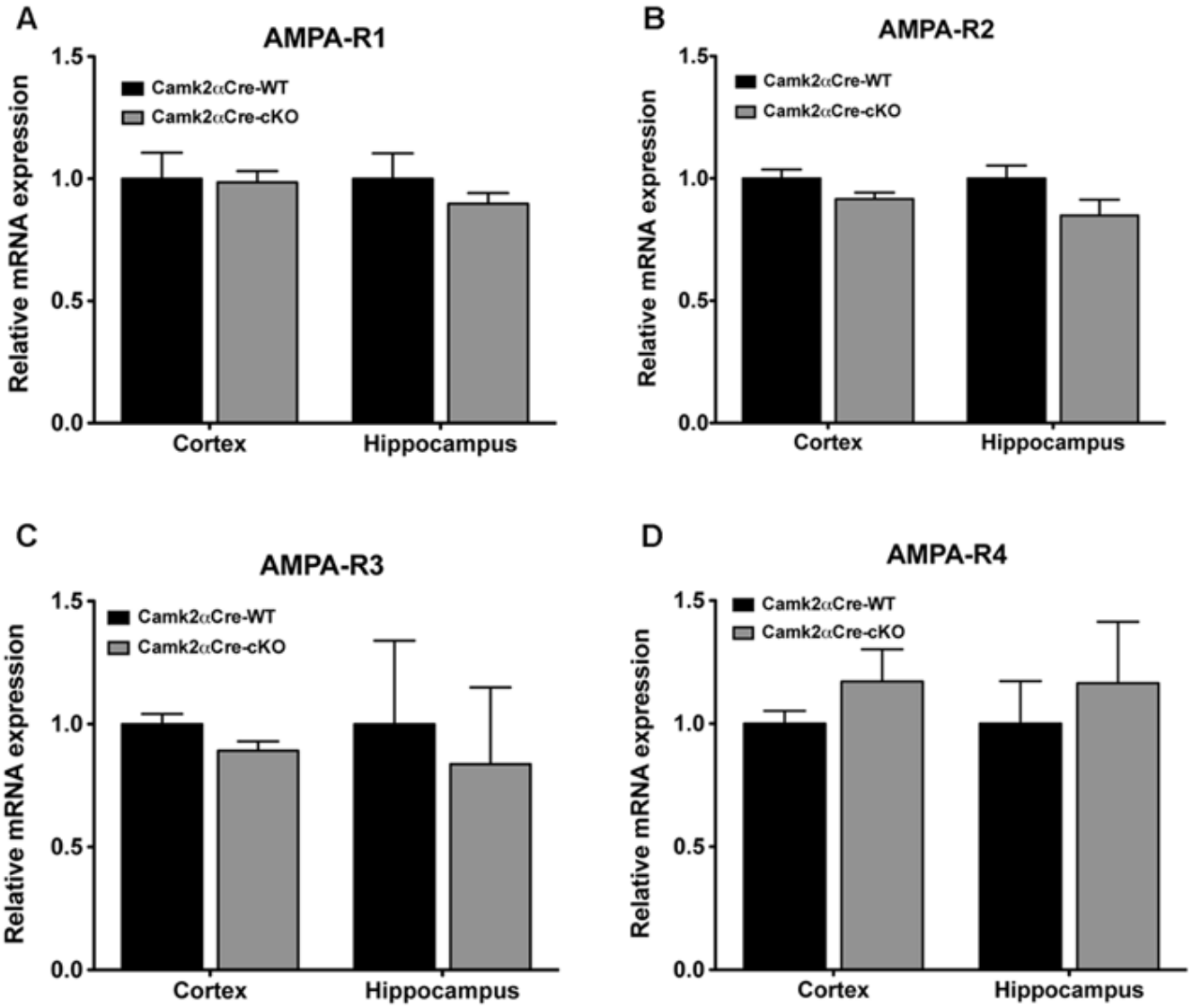

Figure S7. AMPA receptor expression is unchanged in the Camk2αCre-cKO mice. There was no significant difference between the expression of GluR1-4 mRNA in the cortex or hippocampus of the Camk2αCre-cKO mice compared to their WT littermates. (**Cortex**: GluR1: Camk2αCre-WT = 1.0 ± 0.07, *n* = 7; Camk2αCre-cKO = 1.04 ± 0.06, *n* = 7; *p* = 0.805; GluR2: Camk2αCre-WT = 1.0 ± 0.02, *n* = 7; Camk2αCre-cKO = 0.9 ± 0.04, *n* = 7; *p* = 0.180; GluR3: Camk2αCre-WT = 1.0 ± 0.03, *n* = 7; Camk2αCre-cKO = 0.9 ± 0.05, *n* = 7; *p* = 0.165; GluR4: Camk2αCre-WT = 1.0 ± 0.04, *n* = 7; Camk2αCre-cKO = 1.2 ± 0.09, *n* = 7; *p* = 0.456. **Hippocampus**: GluR1: Camk2αCre-WT = 1.0 ± 0.07, *n* = 7; Camk2αCre-cKO = 0.9 ± 0.03, *n* = 7; *p* = 0.456; GluR2: Camk2αCre-WT = 1.0 ± 0.04, *n* = 7; Camk2αCre-cKO = 0.9 ± 0.06, *n* = 7; *p* = 0.259; GluR3: Camk2αCre-WT = 1.0 ± 0.23, *n* = 7; Camk2αCre-cKO = 0.9 ± 0.21, *n* = 7; *p* = 0.945; GluR4: Camk2αCre-WT = 1.0 ± 0.12, *n* = 7; Camk2αCre-cKO=1.2 ± 0.19, *n* = 7; *p* = 0.620. Mann-Whitney, two tailed, all samples were run in duplicate).

Table S1. List of primers used for quantitative polymerase chain reactionexperiments.

Gene Name	Forward Primer (5'-3')	Reverse Primer (5'-3')
Grin1	CGGCTCTTGGAAGATACAGC	GTGAAGTGGTCGTTGGGAGT
GAD67	TGATGGGATATTTTCTCCTGGGG	CGCCATGCCTTTTGTCTTCA
Parvalbumin	ATCAAGAAGGCGATAGGAGCC	GGCCAGAAGCGTCTTTGTT
cholecystokinin	AGCGCGATACATCCAGCAG	ACGATGGGTATTCGTAGTCCTC
somatostatin	GAGCAGGACGAGATGAGGCT	TGGGTTCGAGTTGGCAGAC
DRD1	GCCGCTGTCATCAGGTTTC	GGCCAAAAGCCAGCAATCT
DRD2	CTACTATGCCATGCTGCTCAC	GGCTGACTATCAGGTAGTTGGTG
5HT1A	CCCCAACGAGTGCACCAT	GCGCCGAAAGTGGAGTAGAT
5HT2A	CACTGTGAAGCGAGGCATAA	AAGCCGGAAGTTGTAGCAGA
5HT2B	GTGCCCACAGTTTTCCTAAGG	GGCTCTCTGCTCATTAGAAATGG
5HT2C	TGCCATCGTTTGGGCAATA	CGTCCCTCAGTCCAATCACA
AMPA-R1	CTGTGAATCAGAACGCCTCA	GTTGGCGAGGATGTAGTGGT
AMPA-R2	ATTTCGGGTAGGGATGGTTC	AAAACTGGGAGCAGAAAGCA
AMPA-R3	CGCAGAGCCATCTGTGTTTA	GTTGCCACACCATAGCCTTT
AMPA-R4	TTTGCAGGCAGATTGTCTTG	GGGGCTGGTGTTATGAAGAA

Supplementary References

1. Wang HY, Friedman E (1996): Enhanced protein kinase C activity and translocation in bipolar affective disorder brains. *Biol Psychiatry*. 40:568-575.

2. Ehrlichman RS, Gandal MJ, Maxwell CR, Lazarewicz MT, Finkel LH, Contreras D, *et al.* (2009): N-methyl-d-aspartic acid receptor antagonist-induced frequency oscillations in mice recreate pattern of electrophysiological deficits in schizophrenia. *Neuroscience*. 158:705-712.

3. Gandal MJ, Ehrlichman RS, Rudnick ND, Siegel SJ (2008): A novel electrophysiological model of chemotherapy-induced cognitive impairments in mice. *Neuroscience*. 157:95-104.

4. Halene TB, Ehrlichman RS, Liang Y, Christian EP, Jonak GJ, Gur TL, *et al*. (2009): Assessment of NMDA receptor NR1 subunit hypofunction in mice as a model for schizophrenia. *Genes Brain Behav*. 8:661-675.

5. Lazarewicz MT, Ehrlichman RS, Maxwell CR, Gandal MJ, Finkel LH, Siegel SJ (2010): Ketamine modulates theta and gamma oscillations. *J Cogn Neurosci*. 22:1452-1464.

6. Delorme A, Makeig S (2004): EEGLAB: an open source toolbox for analysis of single-trial EEG dynamics including independent component analysis. *J Neurosci Methods.* 134:9-21.

7. Gandal MJ, Edgar JC, Ehrlichman RS, Mehta M, Roberts TP, Siegel SJ (2010): Validating gamma oscillations and delayed auditory responses as translational biomarkers of autism. *Biol Psychiatry*. 68:1100-1106.

8. Deacon RM, Rawlins JN (2006): T-maze alternation in the rodent. *Nat Protoc*. 1:7-12.

9. Belforte JE, Zsiros V, Sklar ER, Jiang Z, Yu G, Li Y, *et al.* (2010): Postnatal NMDA receptor ablation in corticolimbic interneurons confers schizophrenia-like phenotypes. *Nat Neurosci*. 13:76-83.